Journal of Applied Remote Sensing

RemoteSensing.SPIEDigitalLibrary.org

Lidar methods for measurement of trees in urban forests

Javier Estornell
Borja Velázquez-Martí
Alfonso Fernández-Sarría
Jesús Martí

SPIE.

Javier Estornell, Borja Velázquez-Martí, Alfonso Fernández-Sarría, Jesús Martí, "Lidar methods for measurement of trees in urban forests," *J. Appl. Remote Sens.* **12**(4), 046009 (2018), doi: 10.1117/1.JRS.12.046009.

Lidar methods for measurement of trees in urban forests

Javier Estornell,[a,*] Borja Velázquez-Martí,[b] Alfonso Fernández-Sarría,[a] and Jesús Martí[a]

[a]Universitat Politècnica de València, Departamento de Ingeniería Cartográfica, Geodesia y Fotogrametría, Camino de Vera s/n, València, Spain

[b]Universitat Politècnica de València, Departamento de Ingeniería Rural y Agroalimentaria, Camino de Vera s/n, València, Spain

Abstract. This study compares the estimations of biophysical parameters of *Platanus hispanica* urban trees, namely total height, crown height, crown volume, and the amount of residual biomass from pruning, obtained by terrestrial laser scanner (TLS), airborne laser scanner (ALS) of low density (0.7 points $\cdot$ m^{-2}), and measured by standard field methods. Regression models were calculated to obtain the relationships among parameters retrieved by all techniques, testing all possible combinations (manual-TLS, manual-ALS, TLS-ALS, and vice versa). The most accurate fits were found for vegetation attributes (stem and crown diameter) estimated by TLS and ALS data with R^2 between 0.84 and 0.96, respectively. The least accurate models were found when crown height and pruning biomass were estimated from ALS data ($R^2 = 0.68$ and $R^2 = 0.59$, respectively). The methods reported in this research might be of interest for the management of urban forests to study residual biomass calculation, sink CO_2, the influence of humidity and of shadow areas whatever the information capture system used, whether it is derived from ALS, TLS, or classical dendrometry measurements. © *2018 Society of Photo-Optical Instrumentation Engineers (SPIE)* [DOI: 10.1117/1.JRS.12.046009]

Keywords: terrestrial laser scanner; airborne laser scanner; dendrometry; *Platanus hispanica*.

Paper 180354 received Apr. 28, 2018; accepted for publication Sep. 24, 2018; published online Oct. 23, 2018.

1 Introduction

Vegetation of urban, recreational, industrial, and communication areas has significant ecological and aesthetic functions, helping to improve the quality of urban life. Although urban vegetation was primarily used as a tool for ornamental purposes, nowadays, it is important to focus on its role in improving the environment. The vegetation influences the environmental temperature because the shade prevents the heating of the soil and also the air. It also increases humidity and slows down the action of the wind.[1–3] Finally, it decreases the pollution indicators.[4,5] Studies to estimate the impact of urban forests on environmental quality require structural and tree architecture analysis. In urban zones, the conditions for developing vegetation vary significantly from those that can be found in rural and forest areas. Due to the existence of buildings and pavements, solar irradiation, wind speed, air humidity, and shading, a specific urban microclimate is generated, simultaneously influencing parameters such as the rate of growth and crown shape.[1–3] Some studies have analyzed the costs, benefits, and carbon storage capacity of urban forests.[4,5] Nevertheless, these studies are limited by the lack of research on the amount of biomass contained in urban trees. Moreover, the estimates of carbon storage in urban environments mainly rely upon allometric relationships developed for trees in traditional forests.[4,5] Then to obtain more exact quantification of urban wood biomass, adapted allometric relationships for urban trees are required. Some authors reported the importance of calculating specific allometric equations to estimate biomass stocks in urbans environments to get accurate results.[6–8] The allometry

*Address all correspondence to: Javier Estornell, E-mail: jaescre@cgf.upv.es

1931-3195/2018/$25.00 © 2018 SPIE

associated with traditional forests does not accurately represent urban systems.[9] In addition, equations from literature to estimate parameters of urban trees, very often, are not available or calibrated for these environments.[10] Due to the management actions of urban greenery and planned changes in the spatial structure of green areas within urban community ecosystems, wastes are produced in the form of woody parts that are an annually renewable resource. Recent work reported the possibility of using residual biomass from urban forests, particularly as a renewable energy source or raw material for industry.[11–15]

Characteristics such as low tree density in urban environments, combined with the potential competition for resources, are significant factors for tree development.[9] Growing in an open environment, urban forests frequently receive additional water and nutrient supply. Some studies have shown that urban trees had higher rates of stem growth compared to published rates for the same species in natural forests.[16,17] It is concluded that this is a possible result of release from competition and higher levels of irrigation in addition to precipitation.[17] Trees in urban environments have different challenges comparing to those located in natural forests such as damage, disease, and pruning. Soil moisture, air temperature, relative humidity, leaf temperature, and vapor pressure deficit are less favorable for urban trees.[18]

Direct tree biomass measurement by felling is accurate, but time-consuming, expensive, and forbidden in many environments. For these reasons, destructive sampling is substituted by indirect methods. Plant structure investigation is now focused on the possibility of replacing ground-level labor-intensive inventory practices with modern remote sensing systems. Many studies explored the applicability of terrestrial laser scanning (TLS), airborne laser scanning (ALS), and vehicle-based laser scanning (VLS) for biomass estimation and dimensions measurement at individual plant level.[19–22] These technologies are an observational tool for precise characterization of vegetation architecture within natural and plantation environments. Introduced for applications in urban forests, they allow three-dimensional modeling and geometrical characterization of trees, making it easier to develop management systems based on precise information.

LiDAR (light detection and ranging) data (TLS and ALS systems) have been applied successfully in forestry environments during the last two decades.[23–26] However, in urban forests, few studies have attempted to address these techniques. The classification of individual tree species has been analyzed by combining satellite images and ALS data.[27] In other studies vegetation attributes such as volume, total height, biomass, stem, and crown diameter of urban trees have been studied using ALS data.[28,29] TLS data have been used to retrieve forest inventory variables in urban forests.[30] In forestry, most of the studies with LiDAR data compared only two techniques mainly field-ALS[23–26] and in minor number of cases field-TLS.[31–33] In contrast, stem volume of *Pinus sylvestris L.* and crown biomass of *Norway spruce* were also compared using both ALS and TLS techniques.[22,34] The novelty of our study is that it was focused on estimating dendrometric parameters for *Platanus hispanica* tree, a typical species of Mediterranean trees (few published studies have analyzed this species using airborne LIDAR data), by calculating a set of models to transform dendrometric variables regardless of the available data (TLS, ALS, and field) in an urban environment. In addition, when ALS data are used, there is a crucial parameter to be considered to estimate geometric parameters on single trees, which is data density. The density of ALS data used in previous studies was higher than 4 points m^{-2}.[35–38] Other studies reported that individual tree crowns may be identified from ALS data, if these are dense enough.[39,40] Six to ten hits per tree crown would be required to detect individual trees.[41] Therefore, this study analyzed whether LiDAR data of low density allows to estimate dendrometric variables in an urban environment, where the distribution of trees is regularly separated by the same distance (on both sides of the street and widely spaced) in contrast with the irregularity that can be found in a forest. Another original aspect that is addressed in this paper is the estimation of residual biomass coming from pruning in forest urbans by ALS data. In addition, defining how ALS, TLS, and classical dendrometry variables relate to each other would help to standardize the information of studies that use different techniques. In this way, models obtained from one technique could be applied to obtain parameters of a different technique.

The aim of this work was to calculate a set of regression models to obtain transformations among dendrometric parameters in terms of total and crown height, stem and crown diameter,

crown volume, and the amount of residual biomass from pruning retrieved by all techniques, testing all possible combinations (manual-TLS, manual-ALS, TLS-ALS, and vice-versa). In addition, it was analyzed whether an airborne LiDAR system with a low-point density (0.7 points m^{-2}) is capable of retrieving those parameters. All these analyses were done for *Platanus hispanica* trees, a species widely used in Mediterranean urban areas because it grows rapidly, is resistant to climatic adversities and its measurements allow large areas of shade. These interrelated data can then be applied to studies such as residual biomass calculation, sink CO_2, the influence of humidity and of shadow areas or other—whatever the information capture system used, whether it is derived from ALS, TLS, or classical dendrometry measurements.

2 Materials and Methods

2.1 *Field Study Area*

This study was conducted in Alcúdia, Spain. The study area was defined by a rectangle (Fig. 1) with minimum X, Y (715488, 4341892) and maximum X, Y (715640, 4342178) UTM coordinates (Zone 30S) in the European Terrestrial Reference System 1989 (ETRS89). The climatic parameters of this area are characterized by: average annual temperature 17.8°C, rainfall 454 mm, and humidity 65%. The population of this town is 11,820 inhabitants and the density 473.67 inhabitants $\cdot$ km^{-2}. A set of 30 *Plantanus hispanica* trees were selected being this sample representative of the trees found in Spanish Mediterranean cities according to size, sanitary conditions, and separation.[42] The trees were arranged on an avenue with a traffic flow of ~10,000 vehicles/day. The trees are inside the sidewalk with a separation of 5 m from the buildings. The study area was flat being the slope of the street 0.5% (Fig. 2).

Platanus hispanica has a smooth, narrow stem; its crown forms an oval apparent volume with open branches. Its height can reach 30 m. The selected individuals ranged in total height from 6.4 to 13.3 m; in crown height from 4.1 to 10.7 m; and in crown diameter from 4.1 to 11 m. A set of three trees of the study can be seen in Fig. 3. The trees were arranged on both sides of a road. The mean longitudinal space between sample trees was 20 m and the lateral spacing was ~12 m. This allowed differentiation between selected individuals, which was important for scanning, ground-level observations, and further processing. All individuals were pruned under uniform crown-raising pruning practice after the measuring process had finished. This type of pruning consists of the removal of lower branches in order to provide crown elevation clearance for pedestrian and vehicle traffic and visibility of lights and signs as well.[43]

Fig. 1 Location of study area in Alcúdia (Spain).

(a) (b)

Fig. 2 Characteristics of the urban study area: (a) representation of TLS data and (b) image of the study area.

Fig. 3 Tree numbers 1, 12, and 29 registered by TLS data.

2.2 *Field Measurements*

All measurements were taken during the months of May and June in 2010. Ground-level studies were made to collect *in situ* measurements of the following dimensional properties of sample trees using traditional methods. Diameter at breast height (D_S) outside bark was measured with a traditional aluminum caliper in trees <50 cm in stem diameter or a diameter tape in bigger trees at a point 1.3 m above ground level. Crown diameter (D_C) was measured with a diameter tape and a mirror.[44] Determination of crown diameter at field is complicated due to the irregularity of the crown's outline. The diameter was determined by averaging measurements of the long axis with a diameter taken at right angle.[45–47] Total tree height (H_T) was determined with a Vertex IV (Haglöf) hypsometer. It was measured from the base of the tree to the top of the tallest live portion of the tree crown. Distance from soil to the crown (H_C) was also determined with a Vertex IV hypsometer with precision 0.01 m. This instrument uses ultrasonic pulses together with a transponder fixed to a tree. The tree height was measured from the base of the tree to the top. The apparent volumes of the tree crowns were estimated from crown diameter and height by applying three geometric shapes: cone, paraboloid, and hemisphere.

2.3 *ALS Data*

ALS data used in this study are taken from the publicly available data of the Institut Cartogràfic Valencià of the València region (Spain) and they were acquired during flights between August 5 and September 1 in 2009, using a RIEGL LMS-Q680 sensor. The structure of trees remained practically unchanged between two data campaigns since all trees are pruned every year. The

Fig. 4 Includes the distribution of the ALS data used in this study. The perimeters of crown trees extracted from ALS data are in green.

technical parameters were: pulse frequency 70 kHz, scan frequency 46 Hz, field of view (FOV) 60 deg, and nominal pulse density 0.7 points/m^2; ALS raw data are in LAS files and include the UTM coordinates of the points (x, y, z) in ETRS89. In addition, an LAS file also includes intensity information that corresponds to the energy reflected by objects using near-infrared wavelength. Figure 4 shows the distribution of the ALS data used in this study. Parameters derived from ALS data were obtained using ArcGIS (Esri 2013. ArcGIS Desktop: Release 10.2 Redlands, CA: Environmental Systems Research Institute). To determine the crown of the trees, a digital terrain model (DTM), a digital surface model (DSM), and a canopy height model (CHM) were obtained. The DTM and DSM were calculated by the creation of a terrain dataset. To compute the DTM, the minimum elevations of the original point cloud within a specific size window were selected. Four window sizes were tested to select the most accurate DTM. In these windows, the minimum height was selected.[48] For the assessment of each DTM, 50 true ground points were selected under the canopies. The certainty of the classification of these points was assured since the elevation of close LiDAR points on bare ground was known. Then those points were overlaid onto each DTM and the difference in height was calculated for each point. The points whose difference in height was greater than ± 0.25 m were classified as errors and the points whose difference was lower than ± 0.25 m were classified as ground points. The percentage of points classified correctly was computed for each DTM. The results were for 6×6 m window size, 100%, 4×4 m window size, 98%, 2×2 m, 64%, 1×1 m, 28%. Window sizes of 6×6 m and 4×4 m gave similar accuracy. We selected a 4×4 window size due to the fact that the microrelief of the study is better preserved for smaller windows.[48] Using a 6×6 m window size, one minimum height in 36 m^2 would be selected. For the case of the 4×4 m window size, one minimum point in 16 m^2 was selected. Therefore, it was observed that using a window of 4 m $\times$ 4 m was suitable to select the ground points from the raw ALS data and to discard nonground points (vegetation and vehicle points). This simple method is adequate for open flat areas since ground points can be selected using a relatively small window. The DTM calculated from these points were exported into a raster format using a 1 m $\times$ 1 m pixel size. This cell size was selected to overlap this surface and the DSM calculated using a smaller window size. For DSM, the maximum elevations in a window size of 1 m $\times$ 1 m were selected. The DSM calculated from these points was exported in a raster format using a 1 m $\times$ 1 m pixel size. In this case, larger window sizes generate a more pronounced smoothing effect in the DSM, generating less accurate results. The CHM was obtained by the difference between DSM and DTM.

The CHM was the entry surface to derive crown tree layer. For this process, it was necessary to apply a reclassification process of the CHM considering the thresholds 2.2 and 13.3 m. These

values corresponded to the minimum height of the crown base and the maximum heights of all trees measured at field. All pixels with values within this interval were reclassified as trees. The results of the reclassification corresponded to the projected crown of each *Plantanus hispanica* tree. Then this layer was converted into vector format creating the polygons of the crown (Fig. 4). For other cases, these thresholds can be selected exploring TLS-ALS-field data according the characteristics of the vegetation. For the highest threshold, it is important to remark that this value is not underestimated. The criteria of the maximum height of the trees were right for this study. For the minimum threshold, a value of 2 m is commonly used to eliminate the effect of bushes, stumps, and low-lying vegetation.[49–51] Other authors adjusted this value between 2.4 and 3 m to eliminate the understory vegetation.[52,53] This value also allowed to remove vehicles and urban furniture. The results of using these thresholds allowed to extract the tree crowns in a satisfactory way after overlaying crown features an orthophoto and observing the results of the regression models.

Once the crown polygons were obtained, the area and perimeter were calculated. In addition, the original cloud data point was overlapped considering the polygon crown layer, and those points within each tree were selected. These points were normalized by subtracting the bare-earth surface elevation (i.e., DTM) to every ALS point (tool extract values to points). Then several statistics of the height distribution of points (H_{max}, maximum height; H_{min}, minimum height; H_{mean}, mean height; H_{sd}, standard deviation heights; I_{max}, maximum intensity; I_{min}, minimum intensity; I_{mean}, mean intensity; and I_{sd}, standard deviation intensity) within each tree were obtained using a threshold of 2.2 m to avoid shrub vegetation and vehicles points. Previous studies reported that some statistics derived from intensity LiDAR data provided accurate estimates of biomass.[23,54,55] In our study, it was observed that the correlation coefficient among maximum intensity and stem diameter was 0.67. For total, height tree was 0.59. These results indicated that it should be explored if the metrics derived from intensity LiDAR can improve dendrometric parameter estimations for *Platanus hispanica* trees. All these parameters retrieved from ALS data were potential independent variables to estimate the different dendrometric vegetation attributes of the trees. Maximum height was considered the total height of the tree to perform the analysis. Crown height was calculated by the difference between maximum and minimum heights. Crown diameter was also calculated once the crowns were delineated. To compute the radii of crown trees, several tools of ArcGIS 10.2 were used. The next steps were followed:

1. Entry layer: reclassified CHM with two classes (tree height from 2.2 to 13 m trees, height <2.2 m, and height >13 m no trees).
2. Conversion from raster to polygon layer.
3. Calculate centroids of each polygon.
4. Extract vertices of each polygon in a new layer.
5. Join attributes of crown polygons to crown vertices features using a spatial relationship.
6. Calculate distance among each centroid and vertices for each crown.
7. Calculate the average radii for each crown using the field with the code of each. Then the radius average was calculated and the average diameter was calculated as twice this result.

2.4 *TLS-Data*

A Leica ScanStation2 laser scanner (Heerbrugg, Switzerland) with a dual-axis compensator and the camera resolution was 1 megapixel. The laser scanner was mounted on a tripod and positioned so every tree could be measured without optical obstructions. Specific locations were selected to minimize the influence of obstructing elements. All trees ware scanned at the end of spring (May to June in 2010), when the crowns presented maximum leaf area under calm conditions to limit movement errors caused by wind moving the leaves and branches of the sample tree crowns. Prior to scan acquisition, a minimum of four references or fixed points per station in the form of targets were placed around every sampled tree. These targets were used as ground control points to co-register the *XYZ* point clouds registered from different base stations. A total of 13 base stations were established to measure the 30 sampled trees. From every

station, it was possible to observe more than one tree at a once. Average point spacing among TLS data was 5 mm. Return XYZ point clouds were acquired for all 30 trees and selected for detailed study. Scanning data were processed using Cyclone v.6 (Leica Geosystems AG, Heerbrugg, Switzerland). This software was used to align and merge point clouds and remove points. The accuracy of this process, in terms of absolute mean errors, was between 0.018 and 0.003 m. This software was also used to remove points not belonging to the trees (outliers). After merging data, each tree was recorded in a single file to facilitate processing operations. Several routines were implemented using a software package (MATLAB 7.11, The MathWorks Inc., Natick, Massachusetts, 2010) to compute crown volumes of the trees following the methods Convex Hull (V_{CH}) and Voxel (V_V), total height, crown height, and average diameter.[15,56] The stem diameter was measured directly using 3-D Forest software.

2.5 *Comparison, Estimation of Vegetation Tree Attributes*

The values of total height, crown height, crown diameters, and stem diameters were estimated and the techniques were compared in pairs: field-TLS, field-ALS, and TLS-ALS, and vice versa. Convex hull and voxel volumes obtained from TLS data were related to field and ALS parameters. The relationships between field-TLS data for total height, crown height, crown diameters were already available in Refs. 15 and 56. Equations to relate TLS-ALS, TLS-field, and field-ALS data, and vice versa were obtained in our work. Vegetation attributes such as stem diameter, hemisphere and paraboloid crown volumes, and pruning biomass were predicted from variables derived from ALS and TLS data. Then 14 regression models were calculated for vegetation attributes (D_{SF}, D_{CF}, H_{TF}, H_{CF}, V_H, V_P, B), 7 models using TLS explicative variables, and other 7 ALS variables; 12 models for TLS parameters (D_{STLS}, D_{CTLS}, H_{TTLS}, H_{CTLS}, V_{voxel}, and V_{CH}), 6 models using vegetation attributes, and other 6 ALS data; finally 6 models for ALS data (D_{CALS}, H_{TALS}, and H_{CALS}), 3 models using TLS data, and other 3 models field measurements attributes. The aim is to define a conversion system among biophysical parameters using different capture data. For every dependent variable, a set of models were calculated and the one with the minimum Akaike Information Criterion (AIC) was selected. Multicollinearity in multiregression models was analyzed by means of variance inflation factor (VIF) value. All the models selected had a VIF value under 5.[57] Then for each predicted variable, the regression models were compared using adjusted R^2, RMSE, and AIC values.

3 Results and Discussion

From vegetation attributes measured at field and derived from ALS and TLS data, regression models were calculated for relating the different techniques (field-TLS, field-ALS, and TLS-ALS) (Tables 1–6). Matrices of the models shown in these tables are not symmetric because each model was fitted with the best explanatory variables. Because they are multivariable models, it is not possible to get only one equation to transform the variables of two techniques. So it is necessary to formulate two equations with different input variables. One equation would only be possible when the model obtained has one variable, such as: $\rightarrow D_{STLS} = f^{-1}(D_{SF})$, or $D_{CF} = g(D_{CTLS}) \rightarrow D_{CTLS} = g^{-1}(D_{CF})$. However, when different parameters are involved in the best fit, this is not possible.

3.1 *Stem Diameter D_{SF}*

In Table 2, models obtained to relate stem diameter values measured at field and derived from TLS data with parameters derived by field, TLS, and ALS are shown. Obviously, stem diameter cannot be measured directly by ALS data, which explains the empty row in Table 2. But the capability of ALS data to estimate D_{SF} and D_{STLS} was analyzed using as potential explicative variables those described in Sec. 2.3. In general, this parameter was predicted with high accuracy indicating that field stem diameter can be estimated from TLS and ALS data and TLS stem diameter can be estimated from field data and ALS data as well. As can be observed, the stem diameter obtained in field was better predicted by parameters derived from TLS techniques

Table 1 Parameters analyzed in this study.

Parameter	Description
H_{TTLS}	Tree height measured from TLS data
H_{TALS}	Tree height measured from ALS data
H_{TF}	Tree height measured manually in field
H_{CF}	Crown height measured manually in field
H_{CTLS}	Crown height measured from TLS data
H_{CALS}	Crown height measured from ALS data
$AREA_{ALS}$	Crown area derived from ALS data
$H_{meanALS}$	Mean height of ALS points
H_{sdALS}	Standard deviation height of ALS points
H_{maxALS}	Maximum height of ALS data
H_{minALS}	Minimum height of ALS data
$Int_{meanALS}$	Mean intensity of ALS data
Int_{sdALS}	Standard deviation intensity of ALS data
Int_{maxALS}	Maximum intensity of ALS data
Int_{minALS}	Minimum intensity of ALS data
V_P	Crown volume obtained as a paraboloid calculated from D_{CF} and H_{CF}
V_H	Crown volume obtained as a hemisphere calculated from C_{DF} and H_{CF}
V_{CH}	Crown volume obtained from TLS data by convex hull
V_{VOXEL}	Crown volume obtained from TLS data by voxel calculation
B	Residual biomass
D_{SF}	Stem diameter measured manually in field
D_{STLS}	Stem diameter measured from TLS data
D_{CF}	Crown diameter measured manually in field
D_{CTLS}	Crown diameter measured from TLS data
D_{CALS}	Crown diameter measured from ALS data

(Table 2 and see D_{SF} in Fig. 5). It is important to note that the explanatory parameters were different. TLS data explained 96% of the variability of stem diameter manually measured in the field using as explicative variables crown diameter and tree height. This finding is in line with previous studies indicating the high performance of these variables to predict stem diameter.[58] Appropriate models were also obtained when crown area, mean height, and maximum intensity, derived from ALS data, were used as explicative variables ($R^2 = 0.94$ and RMSE = 1.53 cm). ALS metrics related to the architecture of the tree explained the majority of the variability in this model; but stem diameter prediction improved by 4% when a maximum intensity parameter was added to the model. These results indicate the capability of both sources of data (TLS and ALS) to predict stem diameter, which is particularly interesting in the case of ALS because stem diameter is not registered using this technology. Previous research reported the importance of the stem parameter to predict whole tree biomass and pruning residues. [13,59] Consequently, the results obtained in this study would confirm those results as being of high interest in estimating the biomass of urban forests.

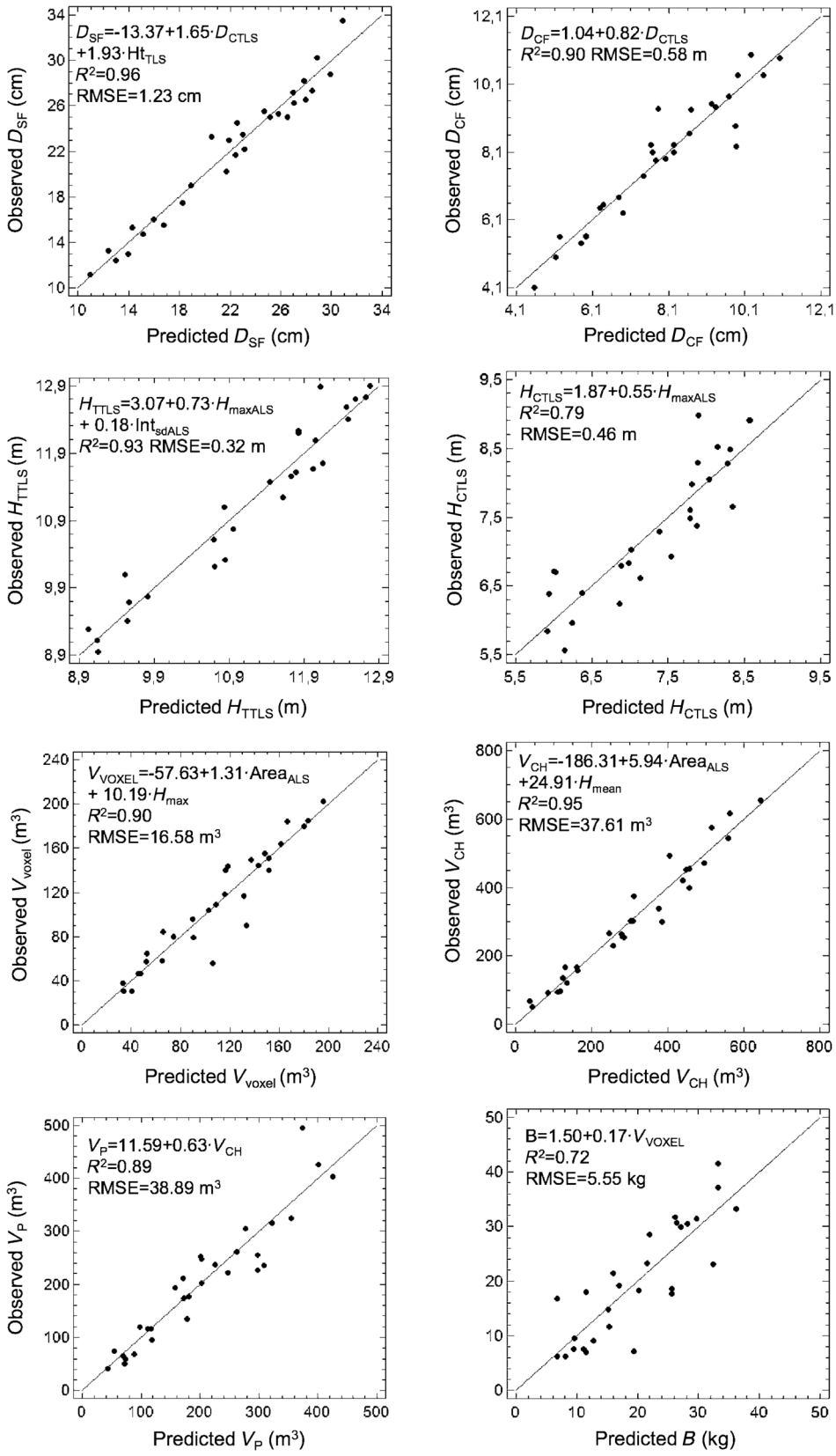

Fig. 5 Best fit models for each variable field stem diameter D_{SF}, field crown diameter D_{CF}, total height obtained by TLS H_{TTLS}, crown height obtained by TLS H_{CTLS}, voxel volume V_{VOXEL}, convex hull volume V_{CH}, paraboloid volume V_P, and biomass B.

Table 2 Models to relate stem diameter measured from different techniques ($p < 0.05$).

	Input		
	Field parameters	TLS parameters	ALS parameters
Field stem diameter	—	$D_{SF} = -13.37 + 1.65 \cdot D_{CTLS} + 1.93 \cdot H_{TTLS}$ $R^2 = 0.96$ RMSE $= 1.23$ cm AIC $= 0.62$	$D_{SF} = -11.15 + 0.12 \cdot \text{area}_{ALS} + 2.28 \cdot H_{meanALS} + 0.35 \cdot \text{Int}_{max}$ $R^2 = 0.94$ RMSE $= 1.53$ cm AIC $= 1.13$
Stem diameter TLS methods	$D_{STLS} = -2.79 + 0.90 \cdot D_{SF} + 1.70 \cdot H_{CF}$ $R^2 = 0.87$ RMSE $= 2.31$ cm AIC $= 1.89$	—	$D_{STLS} = -17.82 + 0.09 \cdot \text{area}_{ALS} + 3.25 \cdot H_{meanALS} + 0.42 \cdot \text{Int}_{max}$ $R^2 = 0.92$ RMSE $= 1.84$ cm AIC $= 1.51$
Stem diameter ALS methods	—	—	—

3.2 *Crown Diameter (D_C)*

Since crown diameter was measured at field and derived from ALS and TLS data, regression models relating the different techniques (field-TLS, field-ALS, TLS-ALS, and vice versa) were calculated (Table 3). These results appear to highlight the ability of ALS data and TLS to predict manually measured crown diameter. R^2 values varied from 0.83 to 0.90. Linear regressions indicated an RMSE between of 0.58 and 0.85 m, which represented between 7% and 11% of the average of all D_C measured in the field, respectively. The most accurate fit was obtained when the field crown diameter was predicted by D_{CTLS} as evidenced by the explained variance being $R^2 = 0.90$ and RMSE $= 0.58$ m (see D_{CF} in Fig. 5), which is 7% of the average of all measured D_C. These findings reconfirm that TLS is the most accurate technique for detecting crown diameters. The beam of divergence and the distance to the target was higher for the ALS system. Consequently, the footprint of the beam of energy in an ALS system is greater than for a TLS system what makes this one more accurate. It is important to point out that the explanatory variable used from TLS data is the crown diameter again. When ALS is used, the explanatory variable selected was crown area. There was also a strong correlation between D_{CTLS} and D_{CALS} ($R^2 = 0.88$ and RMSE $= 0.71$ m). Another aspect worth considering is that with a low density of 0.7 points/m^2 models with determination coefficients higher than 0.84 were obtained. These results could be explained considering the size of the trees (average diameter 8 m) and the regularity of the distribution of the trees (on both sides of the street and widely spaced) in contrast

Table 3 Models to relate crown diameter measured from different techniques ($p < 0.05$).

	Input		
	Field parameters	TLS parameters	ALS parameters
Field crown diameter	—	$D_{CF} = 1.04 + 0.82 \cdot D_{CTLS}$ $R^2 = 0.90$ RMSE $= 0.58$ m AIC $= -0.95$	$D_{CF} = 4.63 + 0.07 \cdot \text{area}_{ALS}$ $R^2 = 0.84$ RMSE $= 0.76$ m AIC $= -0.42$
Crown diameter TLS methods	$D_{CTLS} = -0.37 + 1.10 \cdot D_{CF}$ $R^2 = 0.90$ RMSE $= 0.67$ m AIC $= -0.66$	—	$D_{CTLS} = 4.46 + 0.08 \cdot \text{area}_{ALS}$ $R^2 = 0.88$ RMSE $= 0.76$ m AIC $= -0.41$
Crown diameter ALS methods	$D_{CALS} = 1.08 + 0.31 \cdot \text{Ds}_F$ $R^2 = 0.83$ RMSE $= 0.85$ m AIC $= -0.18$	$D_{CALS} = 4.50 + 0.01 \cdot V_{CH}$ $R^2 = 0.88$ RMSE $= 0.71$ m AIC $= -0.55$	—

with the irregularity we can find in a forest, where a larger point density is necessary. In Fig. 4, the tree crowns extracted from the reclassified CHM can be distinguished. In addition, these findings could be used to upscale limited field or TLS data and create vegetation attribute maps of *Platanus hispanica*.

Another issue that should be considered is the complexity of measuring field crown diameter for large trees in an urban environment.[15] The authors suggested that D_C measured by TLS could be more exact due to the border of the crown, which can be extracted with high detail from the TLS cloud point. From these data, a large number of diameters were extracted by applying a specific algorithm and considering their average as the representative parameter.

3.3 *Tree Height (H_T)*

Models to predict tree height gave very similar R^2 when TLS and ALS data were used, being 0.89 and 0.88, respectively. Both of them use the maximum height as the explanatory variable. In addition, it is important to remark that the highest R^2 (see H_{TTLS} in Fig. 5) was obtained when TLS height of the trees was predicted by parameters of ALS ($R^2 = 0.93$ and RMSE = 0.32 m, around 3% of the average of all tree heights).

In the model based on ALS data, the parameters maximum height and standard deviation of intensity of ALS points were selected as explicative variables. From these variables, the maximum height was the most important explicative variable. For the rest of the models, the values of R^2 varied from 0.81 to 0.93 and the RMSE from 0.32 to 0.70 m (3% to 6% of the average of all tree heights). These results indicate the potential of ALS and TLS systems to predict the height of these trees.

Models to relate TLS and ALS tree height using field measurements had only one variable being the same explanatory parameter (TLS versus field $R^2 = 0.86$; ALS versus field $R^2 = 0.81$; and ALS versus TLS $R^2 = 0.91$). Nevertheless, some relations improved when other variables were considered, as shown in Table 4 (field tree height versus TLS parameters; field tree height versus ALS parameters; and tree height by TLS versus ALS parameters).

3.4 *Crown Height (H_C)*

This is the parameter with the least accurate conversion equations: the values of R^2 varied from 0.68 to 0.83 (Table 5). The RMSE values were higher than those calculated for total height parameters 0.46 to 0.84 m (accounting for around 6% to 11% of average of all field crown heights). These results could be explained by the fact that this parameter is derived from two measurements: maximum tree height and crown base height. So the results can be affected by errors that might occur in either parameter, especially for ALS data, where the maximum

Table 4 Models to relate tree height measured from different techniques ($p < 0.05$).

	Input		
	Field parameters	TLS parameters	ALS parameters
Field tree height	—	$H_{TF} = 2.06 + 0.24 \cdot D_{CTLS} + 0.65 \cdot H_{TTLS}$ $R^2 = 0.89$ RMSE = 0.45 m AIC = −1.39	$H_{TF} = 2.08 + 0.67 \cdot H_{maxALS} + 0.1 \cdot Int_{maxALS}$ $R^2 = 0.88$ RMSE = 0.47 m AIC = −1.29
Tree height TLS methods	$H_{TTLS} = 1.46 + 0.86 \cdot H_{TF}$ $R^2 = 0.86$ RMSE = 0.47 m AIC = −1.37	—	$H_{TTLS} = 3.07 + 0.73 \cdot H_{maxALS} + 0.18 \cdot Int_{sdALS}$ $R^2 = 0.93$ RMSE = 0.32 m AIC = −2.03
Tree height ALS methods	$H_{TALS} = -2.09 + 1.06 \cdot H_{TF}$ $R^2 = 0.81$ RMSE = 0.70 m AIC = −0.56	$H_{TALS} = -3.66 + 1.22 \cdot H_{TTLS}$ $R^2 = 0.91$ RMSE = 0.49 m AIC = −1.26	—

Table 5 Models to relate crown height measured from different techniques ($p < 0.05$).

	Input		
	Field parameters	TLS parameters	ALS parameters
Field crown height	—	$H_{CF} = 2.68 + 0.51 \cdot H_{CTLS} + 0.004 \cdot V_{CH}$ $R^2 = 0.77$ RMSE = 0.61 m AIC = −0.77	$H_{CF} = 1.11 + 0.65 \cdot H_{maxALS}$ $R^2 = 0.68$ RMSE = 0.72 m AIC = −0.50
Crown height TLS methods	$H_{CTLS} = 2.30 + 0.66 \cdot H_{CF}$ $R^2 = 0.70$ RMSE = 0.54 m AIC = −1.08	—	$H_{CTLS} = 1.87 + 0.55 \cdot H_{maxALS}$ $R^2 = 0.79$ RMSE = 0.46 m AIC = −1.41
Crown height ALS methods	$H_{CALS} = -5.24 + 0.008 \cdot V_s + 0.73 \cdot H_{TF}$ $R^2 = 0.81$ RMSE = 0.84 m AIC = −0.13	$H_{CALS}1.30 + 0.01 \cdot V_{CH}$ $R^2 = 0.83$ RMSE = 0.80 m AIC = −0.30	—

height is underestimated and the base crown overestimated, generating a reduction of the crown height.[60] Total and crown heights of the trees were compared calculating the average value for these parameters obtained by each technique. The values for total height were 10.97, 11.11, and 9.84 m for field data, TLS, and ALS, respectively. Clearly, ALS systems underestimate the total height of the trees what could be explained considering the influence of flight height and beam divergence on the canopy point distribution. For crown heights, the values were 7.33, 7.24, and 4.31 m for field data, TLS, and ALS, respectively. The average crown height derived from ALS data was the minimum among the three techniques. For ALS system, this parameter was computed as the difference between maximum height and minimum height. As was described in the introduction, the density of LiDAR data used in this study was 0.7 points $\cdot$ m^{-2}. Most of these points belong to the highest part of the canopy being scarce the number of ALS LiDAR points at the bottom part of it. The high density of branches and leaves generate occlusions, which causes the energy beam does not reach the bottom part of the canopy. These facts may explain the differences found between the average height from the ground to the bottom part of the crown for ALS and field data. For the first case, the value was 5.53 m and for the second case 3.63 m. Therefore, ALS systems show a minor capability to register the bottom part of the canopies, more if we consider the characteristics of the ALS system used in this study. These facts could explain why the field crown height was predicted with lower accuracy from ALS data. On the other hand, for TLS systems, the reference tree height can be affected by limited visibility of the canopy surface from viewpoints on the ground. The difference found in this study, unlike dense forests, is the trees, which are isolated, making it possible to register the external part of the crown with high detail from the different scans.

For TLS crown height estimation by ALS data, maximum height derived from ALS data was selected. Although for this model the R^2 was not the highest ($R^2 = 0.79$), it was selected since the RMSE and AIC value were the lowest.

3.5 *Crown Volume*

The capability of TLS and ALS data to predict field volume can be observed in Table 6. For the paraboloid volume, the best model was obtained when variables derived from TLS data were considered. All the field volumes were best predicted by convex hull volume (see V_P variable in Fig. 5). The values of R^2 decreased slightly when ALS data were used. In particular, the area of the crown was the most significant variable, explaining 82% of the variability of the field volumes. These results reveal the capability of TLS and ALS data to estimate field volumes.

Table 6 Models to relate crown volume measured from different techniques ($p < 0.05$).

	Input		
	Field parameters	TLS parameters	ALS parameters
Field crown volume (semisphere)	—	$V_S = 1.43 + 0.50 \cdot V_{CH}$ $R^2 = 0.85$ RMSE = 35.54 m^3 AIC = 7.27	$V_S = -11.82 + 3.31 \cdot \text{area}_{ALS}$ $R^2 = 0.82$ RMSE = 39.60 m^3 AIC = 7.49
Field crown volume (paraboloid)	—	$V_P = 11.59 + 0.63 \cdot V_{CH}$ $R^2 = 0.89$ RMSE = 38.89 m^3 AIC = 7.45	$V_P = -2.20 + 4.15 \cdot \text{area}_{ALS}$ $R^2 = 0.82$ RMSE = 48.52 m^3 AIC = 7.90
TLS-crown volume (VOXEL)	$V_{VOXEL} = -59.23 + 7.55 \cdot D_{SF}$ $R^2 = 0.79$ RMSE = 23.29 m^3 AIC = 6.43	—	$V_{VOXEL} = -57.63 + 1.31 \cdot \text{area}_{ALS} + 10.19 \cdot H_{max}$ $R^2 = 0.90$ RMSE = 16.58 m^3 AIC = 5.81
TLS-crown volume (CH global)	$V_{CH} = 16.66 + 1.41 V_p$ $R^2 = 0.89$ RMSE = 58.14 m^3 AIC = 8.26	—	$V_{CH} = -186.31 + 5.94 \cdot \text{area}_{ALS} + 24.91 \cdot H_{mean}$ $R^2 = 0.95$ RMSE = 37.61 m^3 AIC = 7.45

The most accurate model to relate TLS crown volume from ALS and field data was obtained for convex hull volume predicted by ALS data. In this case, the mean height and the area of every crown derived by ALS data were selected ($R^2 = 0.95$ and RMSE = 37.61 m^3). For voxel volumes, lower values of R^2 were obtained when they were related to ALS parameters ($R^2 = 0.90$) or field variables ($R^2 = 0.79$). Here, the capability of ALS parameters to predict voxel volumes of the crown derived from TLS data should be emphasized. This variable, as will be seen in the next section, was well correlated with the residual biomass of the crown. These results reveal the lower ability of field measurements to predict TLS volume.

3.6 *Residual Biomass (B)*

The best model to predict residual biomass was found when the voxel volume derived from TLS data was used (Table 7); $R^2 = 0.72$ and RMSE = 5.55 kg, which accounts for 28% of the average of residual biomass per tree. This result indicates the explanatory power of this variable for predicting residual biomass of *Platanus hispanica*. A significant decrease in terms of R^2 and larger values of RMSE were observed when this variable was predicted by ALS data ($R^2 = 0.59$, RMSE = 6.73 kg, and 34% of the average of all residual biomass per tree). This result reveals the lower capability of ALS data of low resolution to predict this variable. Nevertheless, some findings reveal high correlations between area of the crown derived from ALS data and residual pruning from agricultural systems.[60] Further research is required here to analyze if higher density of ALS data can improve this estimation.

Table 7 Models to relate pruning residues measured from different techniques ($p < 0.05$).

	Input	
	TLS parameters	Field parameters
Field pruning residues	$B = 1.50 + 0.17 \cdot V_{VOXEL}$ $R^2 = 0.72$ RMSE = 5.55 kg AIC = 3.57*	$B = -28.44 + 4.91 \cdot H_{maxALS}$ $R^2 = 0.59$ RMSE = 6.73 kg AIC = 3.96

4 Conclusions

The capability of TLS and ALS data to predict biophysical parameters obtained by standard field methods was demonstrated in this study for *Platanus hispanica*. In general, models obtained from ALS data gave less accurate predictions. Despite the low density of ALS data used in this study, this technology can be considered as alternative to predict vegetation attributes of urban forests. In addition, one of the advantages that ALS offers is the larger area that can be covered at a lower cost financially and in time in contrast to TLS techniques. It is expected that by using larger density of ALS data, these results can improve. Models that allow researchers to transform parameters derived from TLS data to ALS data and from ALS to TLS have also been obtained in this study and this could be used in other areas where there are ALS data (these data are available in the whole territory of some countries). It should be highlighted that the most accurate fits for TLS parameters associated to the height were found when they were predicted from ALS data. However, pruning biomass estimation requires further research to test the capability of ALS data to predict this variable.

TLS variables have enormous potential in estimating biophysical variables. The TLS measures offer great precision due to the density of points registered, which allows the structure of the crown to be detected in more detail. Therefore, the results obtained in this study could be used to transform TLS parameters using ALS data or vegetation attributes obtained at fields of lower accuracy.

References

1. G. M. Heisler, R. H. Grant, and W. Gao, "Urban tree influences on ultraviolet irradiance," *Proc. SPIE* **4482**, 277–290 (2002).
2. H. R. Na et al., "Modeling of urban trees' effects on reducing human exposure to UV radiation in Seoul, Korea," *Urban For. Urban Greening* **13**(4), 785–792 (2014).
3. H. Takebayashi et al., "Analysis of solar radiation shading effects by trees in the open space around buildings," *Sustainability* **9**(8), 1398 (2017).
4. E. G. McPherson and J. R. Simpson, "Carbon dioxide reductions through urban forestry: guidelines for professionals and volunteer tree planters," PSW GTR-171, USDA Forest Service, Pacific Southwest Research Station, Center for Urban Forest Research, Albany (2001).
5. D. E. Pataki et al., "Urban ecosystems and the North American carbon cycle," *Global Change Biol.* **12**(11), 2092–2102 (2006).
6. E. Aguaron and E. G. McPherson, "Comparison of methods for estimating carbon dioxide storage by Sacramento's urban forest," Chapter 3 in *Carbon Sequestration in Urban Ecosystems*, R. Lal and B. Augustin, Eds., pp. 43–70, Springer, New York (2012).
7. E. G. McPherson and P. J. Peper, "Urban tree growth modeling," *J. Arboric. Urban For.* **38**(5), 172–180 (2012).
8. S. F. López-López et al., "Non-destructive method for above-ground biomass estimation of *Fraxinus uhdei* (Wenz.) Lingelsh in an urban forest," *Urban For. Urban Greening* **24**, 62–70 (2017).
9. M. R. McHale et al., "Urban forest biomass estimates: is it important to use allometric relationships developed specifically for urban trees?" *Urban Ecosyst.* **12**, 95–113 (2009).
10. C. Dobbs, J. Hernández, and F. Escobedo, "Above ground biomass and leaf area models based on a non destructive method for urban trees of two communes in Central Chile," *Bosque* **32**(3), 287–296 (2011).
11. B. Velázquez-Martí et al., "Wood characterization for energy application proceeding from pruning Morus alba L., *Platanus hispanica* Münchh and *Sophora japonica* L. in urban areas," *Renewable Energy* **62**, 478–483 (2014).
12. B. Velázquez-Martí et al., "Prediction and evaluation of biomass obtained from citrus trees pruning," *J. Food Agric. Environ.* **11**(3–4), 1485–1491 (2013).
13. M. Sajdak, B. Velázquez-Martí, and I. López-Cortés, "Quantitative and qualitative characteristics of biomass derived from pruning *Phoenix canariensis* hort. ex Chabaud. and *Phoenix dactilifera* L.," *Renewable Energy* **71**, 545–552 (2014).

14. M. Sajdak et al., "Prediction models for estimating pruned biomass obtained from *Platanus hispanica* Münchh. used for material surveys in urban forests," *Renewable Energy* **66**, 178–184 (2014).
15. A. Fernández-Sarría et al., "Residual biomass calculation from individual tree architecture using terrestrial laser scanner and ground-level measurements," *Comput. Electron. Agric.* **93**, 90–97 (2013).
16. A. Moser et al., "Inter- and intraannual growth patterns of urban small-leaved lime (*tilia cordata* mill.) at two public squares with contrasting microclimatic conditions," *Int. J. Biometeorol.* **61**(6), 1095–1107 (2017).
17. R. W. Rhoades and R. J. Stipes, "Growth of trees on Virginia Tech campus in response to various factors," *J. Arboric.* **25**(4), 211–217 (1999).
18. E. N. M. Inkiläinen et al., "The role of the residential urban forest in regulating throughfall: a case study in Raleigh, North Carolina, USA," *Landscape Urban Plann.* **119**, 91–103, (2013).
19. Y. Lin et al., "From TLS to VLS: biomass estimation at individual tree level," *Remote Sens.* **2**, 1864–1879 (2010).
20. H. Kaartinen et al., "An international comparison of individual tree detection and extraction using airborne laser scanning," *Remote Sens.* **4**(4), 950–974 (2012).
21. W. Li et al., "A new method for segmenting individual trees from the lidar point cloud," *Photogramm. Eng. Remote Sens.* **78**, 75–84 (2012).
22. M. Hauglin et al., "Estimating single-tree crown biomass of Norway spruce by airborne laser scanning: a comparison of methods with and without the use of terrestrial laser scanning to obtain the ground reference data," *Forests* **5**(3), 384–403 (2014).
23. M. García et al., "Estimating biomass carbon stocks for a Mediterranean forest in central Spain using LiDAR height and intensity data," *Remote Sens. Environ.* **114**(4), 816–830 (2010).
24. M. Van Leeuwen and M. Nieuwenhuis, "Retrieval of forest structural parameters using LiDAR remote sensing," *Eur. J. For. Res.* **129**(4), 749–770 (2010).
25. R. Valbuena, M. Maltamo, and P. Packalen, "Classification of forest development stages from national low-density lidar datasets: a comparison of machine learning methods," *Rev. Teledetección* **45**, 15–25 (2016).
26. A. Hevia et al., "Modelling canopy fuel and forest stand variables and characterizing the influence of thinning in the stand structure using airborne LiDAR," *Rev. Teledetección* **45**, 41–55 (2016).
27. C. Zhang and F. Qiu, "Mapping individual tree species in an urban forest using airborne lidar data and hyperspectral imagery," *Photogramm. Eng. Remote Sens.* **78**, 1079–1087 (2012).
28. R. Hecht, G. Meinel, and M. F. Buchroithner, "Estimation of urban green volume based on single-pulse LiDAR data," *IEEE Trans. Geosci. Remote Sens.* **46**(11), 3832–3840 (2008).
29. R. Shrestha and R. H. Wynne, "Estimating biophysical parameters of individual trees in an urban environment using small footprint discrete-return imaging Lidar," *Remote Sens.* **4**(2), 484–508 (2012).
30. L. M. Moskal and G. Zheng, "Retrieving forest inventory variables with terrestrial laser scanning (TLS) in urban heterogeneous forest," *Remote Sens.* **4**(1), 1–20 (2012).
31. P. J. Wat and D. N. M. Donoghue, "Measuring forest structure with terrestrial laser scanning," *Int. J. Remote Sens.* **26**(7), 1437–1446 (2005)
32. H.-G. Maas et al., "Automatic forest inventory parameter determination from terrestrial laser scanner data," *Int. J. Remote Sens.* **29**(5), 1579–1593 (2008)
33. K. Calders et al., "Nondestructive estimates of above ground biomass using terrestrial laser scanning," *Meth. Ecol. Evol.* **6**, 198–208 (2015)
34. V. Kankare et al., "Accuracy in estimation of timber assortments and stem distribution—a comparison of airborne and terrestrial laser scanning techniques," *ISPRS J. Photogramm. Remote Sens.* **97**, 89–97 (2014).
35. X. Yu et al., "Automatic detection of harvested trees and determination of forest growth using airborne laser scanning," *Remote Sens. Environ.* **90**(4), 451–462 (2004)

36. S. Solberg, E. Naesset, and O. M. Bollandsas, "Single tree segmentation using airborne laser scanner data in a structurally heterogeneous spruce forest," *Photogramm. Eng. Remote Sens.* **72**, 1369–1378 (2006).
37. J. Vauhkonen et al., "Imputation of single-tree attributes using airborne laser scanning-based height, intensity, and alpha shape metrics," *Remote Sens. Environ.* **114**(6), 1263–1276 (2010).
38. C. Straub and B. Koch, "Estimating single tree stem volume of *pinus sylvestris* using airborne laser scanner and multispectral line scanner data," *Remote Sens.* **3**(5), 929–944 (2011).
39. J. Hyyppä and M. Inkinen, "Detecting and estimating attributes for single trees using laser scanner," *Photogramm. J. Finl.* **16**, 27–42 (1999).
40. E. Lindberg and M. Hollaus, "Comparison of methods for estimation of stem volume, stem number and basal area from airborne laser scanning data in a hemi-boreal forest," *Remote Sens.* **4**(4), 1004–1023 (2012).
41. S. Magnussen, P. Eggermonth, and V. La Riccia, "Recovering tree heights from airborne laser scanner data," *For. Sci.* **45**, 407–422 (1999).
42. A. F. Davila et al., "Mapping the sources of urban dust in a coastal environment by measuring magnetic parameters of *Platanus hispanica* leaves," *Environ. Sci. Technol.* **40**(12), 3922–3928 (2006).
43. P. Alcázar et al., "Airborne plane-tree (Platanus hispanica) pollen distribution in the city of Córdoba, South-Western Spain, and possible implications on pollen allergy," *J. Invest. Allergol. Clin. Immunol.* **14**(3), 238–243 (2004).
44. T. E. Avery and H. E. Burkhart, *Forest Measurements*, 5th ed., p. 456, Waveland Press, Inc., Long Grove, Illinois (2015).
45. B. Husch, T. W. Beers, and J. A. Kershaw, *Forest Mensuration*, 4th ed., John Wiley and Sons, Inc., New York (2003).
46. M. Court-Picon et al., "Dendrometry and morphometry of *Pinus pinea* L. in Lower Provence (France): adaptability and variability of provenances," *For. Ecol. Manage.* **194**(1–3), 319–333 (2004).
47. P. W. West, *Tree and Forest Measurement*, Springer-Verlag, Berlin, Heidelberg (2009).
48. J. Estornell et al., "Analysis of the factors affecting LiDAR DTM accuracy in a steep shrub area," *Int. J. Digital Earth* **4**, 521–538 (2011).
49. M. V. N. d'Oliveira et al., "Estimating forest biomass and identifying low-intensity logging areas using airborne scanning LiDAR in Antimary State Forest, Acre State, Western Brazilian Amazon," *Remote Sens. Environ.* **124**, 479–491 (2012).
50. S. E. Reutebuch, H.-E. Andersen, and R. J. McGaughey, "Light detection and ranging (LIDAR): an emerging tool for multiple resource inventory," *J. For.* **103**(6), 286–292 (2005).
51. S. C. Popescu, R. H. Wynne, and R. F. Nelson, "Estimating plot-level tree heights with LiDAR: local filtering with a canopy-height based variable window size," *Comput. Electron. Agric.* **37**(1–3), 71–95 (2002).
52. E. Næsset, "Accuracy of forest inventory using airborne laser scanning: evaluating the first Nordic full-scale operational project," *Scand. J. For. Res.* **19**(6), 554–557 (2004).
53. Y. Kim et al., "Distinguishing between live and dead standing tree biomass on the North Rim of Grand Canyon National Park, USA using small-footprint LiDAR data," *Remote Sens. Environ.* **113** (11), 2499–2510 (2009).
54. J. A. N. Van Aardt, R. H. Wynne, and R. G. Oderwald, "Forest volume and biomass estimation using small-footprint lidar-distributional parameters on a per-segment basis," *For. Sci.* **52**(6), 636–649 (2006).
55. J. Estornell et al., "Estimation of biomass and volume of shrub vegetation using LiDAR and spectral data in a Mediterranean environment," *Biomass Bioenergy* **46**, 710–721 (2012).
56. A. Fernández-Sarría et al., "Different methodologies for calculating crown volume of *Platanus hispanica* trees by terrestrial laser scanner and comparison with classical dendrometric measurements," *Comput. Electron. Agric.* **90**, 176–185 (2013).
57. P. A. Rogerson, *Statistical Methods for Geography*, SAGE, London (2001).

58. S. C. Popescu, "Estimating biomass of individual pine trees using airborne Lidar," *Biomass Bioenergy* **31**, 646–655 (2007).
59. B. Velázquez-Martí, M. Sajdak, and I. López-Cortés, "Available residual biomass obtained from pruning of Morus alba L. trees cultivated in urban forest," *Renewable Energy* **60**, 27–33 (2013).
60. J. Estornell et al., "Estimation of pruning biomass of olive trees using airborne discrete-return LiDAR data," *Biomass Bioenergy* **81**, 315–321 (2015).

Javier Estornell is an associate professor at the Universitat Politècnica de València, Spain, where he teaches remote sensing and geographical information systems. He is a member of the GeoEnvironmental Cartography and Remote Sensing Group of this university. Since 2014, he has been an assistant editor of the *Spanish Journal of Remote Sensing*. His research interests focus on the application of LiDAR data and satellite images in agriculture, forestry, and coast studies.

Borja Velázquez-Martí received his PhD from the Universitat Politècnica de València, Spain, where he teaches agricultural mechanization and bioenergy in the Department of Rural and Food Engineering. His research work is focused on quantification, logistics, and management of biomass for energy. He is a coauthor of more than 50 scientific articles in the *Journal Citation Report*. He has authored five books.

Alfonso Fernández-Sarría is an associate professor at the Universitat Politècnica de València, Spain, teaching applied remote sensing and geomorphology. He is a member of the GeoEnvironmental Cartography and Remote Sensing Group. Since 2017, he has been an academic director of the master's degree in geomatics engineering and geoinformation. His research interests focus on processing airborne and terrestrial LiDAR and multispectral and RADAR imagery to manage coastal, forestry, and agricultural areas.

Jesús Martí is an associate professor at the Universitat Politècnica de València, Spain, where he teaches cartography, GIS, and remote sensing. He is a member of the Research Institute for Integrated Management of Coastal Areas. Since 2017, he has been an academic director of the bachelor's degree in environmental sciences. His research focuses on the application of LiDAR data and satellite images in studies related to agriculture, forestry, and coasts.